




Article

Effects of *TaMTL*-Edited Mutations on Grain Phenotype and Storage Component Composition in Wheat

Huali Tang^{1,2}, Shuangxi Zhang³, Mei Yu¹, Ke Wang¹ , Yang Yu⁴, Yuliang Qiu¹, Yanan Chang¹, Zhishan Lin¹, Lipu Du¹, Daolin Fu⁵, Zichao Li^{2,*}  and Xingguo Ye^{1,*} 

- ¹ Institute of Crop Science, Chinese Academy of Agricultural Sciences, Beijing 100081, China; tanghuali1990@163.com (H.T.); ym17852022302@163.com (M.Y.); wangke03@caas.cn (K.W.); mhsqyl@163.com (Y.Q.); yananchang1992@163.com (Y.C.); linzhishan@caas.cn (Z.L.); dulipu@caas.cn (L.D.)
- ² College of Agronomy, China Agricultural University, Beijing 100193, China
- ³ Crop Research Institute, Ningxia Academy of Agri-Forestry Sciences, Yinchuan 750105, China; shxzhang@163.com
- ⁴ School of Agriculture, Yangtze University, Jingzhou 434000, China; yuyangyang4569@163.com
- ⁵ State Key Laboratory of Crop Biology, College of Agronomy, Shandong Agricultural University, Taian 271018, China; dlfd@sdau.edu.cn
- * Correspondence: lizichao@cau.edu.cn (Z.L.); yexingguo@caas.cn (X.Y.); Tel./Fax: +86-10-62731414 (Z.L.); +86-10-821015173 (X.Y.)

Abstract: Wheat nutrition and processing-quality are primarily based on the endosperm ingredients. However, the effect of embryos on grain traits and components remains unclear. In this study, we found that in the cross-pollinated and self-pollinated progenies of the four wheat *mtl* mutants (*mtl-A*, *mtl-AD*, *mtl-BD*, and *mtl-ABD*) the haploid induction rates were 0–15.6% and 0–14.1%, and the embryo abortion rates were 0–27.4% and 0–24.1%, respectively, in which *mtl-A* had no effect on haploid induction and embryo development. The embryoless grains (ELG) were comparable to the normal grains (NG) from *mtl-AD*, *mtl-BD*, and *mtl-ABD* in grain length, grain width and thousand-kernel weight, but the grain traits were significantly less than those in NG from mutant *mtl-A*. During grain filling period, *mtl-ABD* had similar ELG ratio and amount of starch granule (SG) and protein body (PB) in ELG and NG. At maturity stage, the morphological features of A-type and B-type SG in ELG were similar to those in NG in *mtl* mutants; however, amylose, gliadin, and glutenin contents were higher in ELG, and total starch, albumin and globulin contents were higher in NG. Our results clarified the effect of the wheat *mtl* mutants on haploid induction and grain traits and nutrition composition in this crop, and provided new clues for studying the development of embryo and endosperm and their interaction in plants.

Keywords: wheat *TaMTL* gene; haploid induction rate; grain botanic and quality traits



Citation: Tang, H.; Zhang, S.; Yu, M.; Wang, K.; Yu, Y.; Qiu, Y.; Chang, Y.; Lin, Z.; Du, L.; Fu, D.; et al. Effects of *TaMTL*-Edited Mutations on Grain Phenotype and Storage Component Composition in Wheat. *Agriculture* **2022**, *12*, 587. <https://doi.org/10.3390/agriculture12050587>

Academic Editor: Jaime Prohens

Received: 5 March 2022

Accepted: 20 April 2022

Published: 22 April 2022

Publisher's Note: MDPI stays neutral with regard to jurisdictional claims in published maps and institutional affiliations.



Copyright: © 2022 by the authors. Licensee MDPI, Basel, Switzerland. This article is an open access article distributed under the terms and conditions of the Creative Commons Attribution (CC BY) license (<https://creativecommons.org/licenses/by/4.0/>).

1. Introduction

Seeds are the most important organ for plant reproduction and human nutrition. A seed normally contains three parts: a diploid embryo, a triploid endosperm, and the seed coat. A diploid embryo is formed by fusing one egg cell and one sperm cell [1]; a triploid endosperm is formed by fusing two central nuclei and one sperm cell. The seed coat is a diploid tissue of the mother plant and protects the embryo and endosperm [2,3]. In plant kingdom, the proportion of embryo and endosperm in seeds is different, but it is genetically fixed for plants of the same species [4,5]. In maize, the starchy endosperm accounts for 77.8% weight of a mature kernel. In rice, the starchy endosperm represents nearly 91% of dry matters of a mature seed excluding hull, and the embryo explains about 3% dry matters [2]. Common wheat (*Triticum aestivum* L., $2n = 6X = 42$, AABBDD) is one of the largest cereal crops. Worldwide, an annual production of wheat is approximately seven million tons, which secures food supplies for nearly 40% of the human population,

providing about 21% of calories and 20% of proteins consumed by human kind [6]. In wheat seeds, the starchy endosperm accounts for 83–84% of dry matters, while embryo represents only a fraction of 3% [7]. In mature seeds of wheat, the embryos contain high levels of lipids and fat-soluble vitamins, and they germinate into radicle, germ, and finally an entire plant [2]. The wheat endosperm reserves about 65–75% starch and 10–15% protein of the final dry weight [8,9] of which the starch contains 70–80% amylopectin and 20–30% amylose. Amylopectin is highly branched and more easily digested and absorbed by humans, while amylose has few branches and tends to form indigestible complexes [10–12].

In wheat, there are two types of starch granules: large granules (A-type, 10–35 μm in diameter) and small granules (B-type, 1–10 μm in diameter) [13]. A-type granules are either lenticular or spherical in appearance, and B-type granules are either spherical or polygonal. The A- and B-type granules accounts for 70% and 30% of the total volume of an endosperm, respectively [14,15]. Sometimes, the B-type granules are divided into an intermediate type (B, 9–11 μm in diameter) and small type (C, 2–3 μm in diameters) [16]. The seeds have four types of storage proteins: albumins (soluble in water), globulins (insoluble in water, but soluble in salt solution), gliadins (soluble in ethanol), and glutenins (soluble in acid and base solution). Albumins and globulins primarily contain proteases [17]. Gliadins and glutenins together account for 60–80% of the total grain protein [18,19], these proteins are associated with the adhesion and viscoelasticity of dough, which are required functional components for making noodles, bread and other baked goods [9,20]. Gliadins are monomeric storage proteins, including alpha, gamma and omega gliadins [21,22]. Glutenins have both high molecular weight glutenin subunits (HMW-GSs, 66–88 kDa) and low molecular weight glutenin subunits (LMW-GSs, 32–45 kDa), which together form polymeric proteins ranging from 150 kDa to over 1500 kDa in molecular weight [23–26].

The *MATRILINEAL* (*MTL*) encodes a sperm phospholipase and controls haploid induction (HI) in maize [27]. A frameshift mutation in the maize *ZmPLA1* (*ZmMTL*) gene induces haploid seed production in both self- and cross-pollinated progenies [25]. The CRISPR/Cas9-based disruption of *ZmPLA1* caused a 3.7% and 6.7% haploid induction rate (HIR) in the heterozygous and homozygous mutants, respectively, in the self-pollinated progenies, and 1.9–3.5% haploid induction rates (HIR) in the heterozygous mutant and 1.6% HIR in the homozygous mutant in the cross-pollinated progenies; surprisingly, embryo abortion occurs to 14.3% self-pollinated kernels and 10% cross-pollinated F_1 kernels in which the mutation lines were used as pollen donors [28]. The *MTL* gene is highly conserved in rice (*Oryza sativa* L.), wheat, barley (*Hordeum vulgare* L.), and other cereal crops [28]. When the rice *OsMTL* gene was disrupted by CRISPR/Cas9, there was a 20% seed setting rate (SSR) and a 6% HIR in the self-pollinated seeds of the edited mutants [29]. In wheat, the *TaPLA* double mutations in the A and D genomes (same as *mtl-AD*) caused a 30–60% SSR and a 5.9–15.7% HIR in the self-pollinated progenies [30]. We also discovered that the wheat *mtl* mutations were associated with about 10–31.6% HIR and many embryoless grains (ELG) in the self-pollinated progenies [31].

However, it is unclear if the mutation locus and embryo abortion affect HIR, grain traits and endosperm components in the CRISPR/Cas9-based wheat *mtl* mutants. To clarify the effect of the wheat *mtl* mutants on haploid induction and grain traits and nutrition composition, we here will characterize the HIR, grain morphology, ELG dynamic change, and relative non-gluten, gluten, and starch compositions in the *mtl* mutants in wheat. The study will shed new light into a coordinated growth between embryo and endosperm in wheat and provides valuable data for breeding and food industry.

2. Materials and Methods

2.1. Wheat Materials and Planting

Previously, we edited the *MTL* alleles in a wheat cultivar “Felder” using CRISPR/Cas9 by *Agrobacterium*-mediated genetic transformation and generated a diversity of wheat *mtl* mutants [31], from which we further developed four wheat *mtl* mutants: (1) *mtl-A* with homozygous mutation in the genome A allele (having a 1-bp insertion at targeting site

TaMTL-4A-gM471), (2) *mtl-AD* with homozygous mutations in A (having a 1-bp insertion at targeting site *TaMTL-4A-gM471*) and D (having a 1-bp deletion at targeting site *TaMTL-4D-gM179*) alleles, (3) *mtl-BD* with homozygous mutations in B (having a 1-bp insertion at targeting site *TaMTL-4B-gM179*) and D (having a large fragment deletion of 292 bp between the targets *TaMTL-4D-gM179* and *TaMTL-4D-gM471*) alleles, and (4) *mtl-ABD* with homozygous mutations in all A (having a 291-bp deletion between the targets *TaMTL-4A-gM179* and *TaMTL-4A-gM471*), B (having a large fragment deletion of 291 bp between the targets *TaMTL-4B-gM179* and *TaMTL-4B-gM471*) and D (having a 1 bp deletion at *TaMTL-4D-gM179*) alleles. The mutant plants contained the *bar* and *Cas9* expression cassettes. The cultivar “Fielder” used as a control in this study was kindly provided by Japan Tobacco Company (Iwata, Japan).

Wheat materials were planted and secured at the Experimental Station of Institute of Crop Sciences (ICS), Chinese Academy of Agricultural Sciences (CAAS), Beijing, China, in February in 2021 with a 1.5 m length and 20 cm width. At heading stage, 25 plants from each mutant type were used as male parents to be crossed with wild type “Fielder” for generating F₁ hybrid grains, and another 25 plants from each mutant were tagged for flowering date for obtaining self-pollinated grains at different stage. Developing grains were collected from central spikelets at 9, 12, 15, 18, 23 and 28 days post anthesis (DPA) (approximately 300 grains per time course). The ELG and endospermless grains (EnLG) were analyzed using a stereoscopic microscope (HT7700, Hitachi Limited, Tokyo, Japan).

2.2. Embryo Rescue from Endospermless Grains

The immature EnLG were identified from harvested grains, sterilized with 70% ethanol for 1 min and 4% sodium hypochlorite for 5 min, and rinsed three times with sterile water. Immature embryos were isolated under a stereoscopic microscope, maintained on a half MS medium (plus 20 g L⁻¹ sucrose and 2.4 g L⁻¹ phytigel, pH 5.8) in darkness at 25 °C for 3 d, and then shifted to a photoperiod of 16h-light/8h-darkness condition (120 μmol m⁻² s⁻¹) at 25 °C for two weeks. Rescued seedlings were then transplanted into soil and grown in a climate chamber (25 °C, 16h-light/8h-darkness with an intensity of 300 μmol m⁻² s⁻¹).

2.3. Determination of Wheat Guard Cell Length

Leaves of 2 cm length were collected from the rescued main tillers at the jointing stage, and placed with the abaxial side facing up on a glass slide. Mesophyll tissues were gently removed to form a clear epidermis [32]. Ten guard cells per plant were analyzed under a light microscope (BX51, Olympus Corporation, Tokyo, Japan).

2.4. Chromosome Counting in Wheat Root Tips

Chromosome squashing was performed by a published method [33,34]. Seeds were germinated in petri dishes at 25 °C under darkness for 2–3 d. When roots reached 2–3 cm long, root tips (ca. 1cm) were treated with nitrous oxide for 2 h, fixed in 90% acetic acid for 5 min, and then washed three times with sterile water. Milky tips of the treated roots were further processed by enzymolysis liquid (cellulase, pectinase and macerozyme, 2:2:1 in weight). Chromosomes were inspected under a light microscope (BX51, Olympus Corporation, Japan).

2.5. Marker-Assisted Haploid Confirmation in Hybrid F₁ Seedlings

Hybrid F₁ plant DNA was extracted by the FastPure Plant DNA Kit (Vazyme Biotech Co., Ltd., Nanjing, China). Diagnostic fragments of 430 bp and 706 bp were used to confirm the presence of *bar* and *Cas9* genes in the F₁ plants using the specific primer pairs (Table 1). A 20 μL PCR reaction included 10 uL 2 × Taq MasterMix (Vazyme Biotech), 0.5 μL of each primer (10 μM), 8 μL ddH₂O, and 1 μL genomic DNA (100 ng μL⁻¹). PCR condition for *bar* was 95 °C for 5 min, 28 cycles of 95 °C for 30 s, 28 °C for 30 s, 72 °C for 30 s, and a 10 min extension at 72 °C. PCR condition for *Cas9* was 95 °C for 5 min, 35 cycles of 95 °C

for 30 s, 56 °C for 30 s, 72 °C for 40 s, and a 10 min extension at 72 °C. The PCR products were separated in a 2% (*w/v*) agarose gel and observed under UV light.

Table 1. The PCR primers used in this study.

Primer Name	Primer Sequence (5' → 3')	Product Size (bp)	Application
<i>bar</i> -F <i>bar</i> -R	ACCATCGTCAACCACTACATCG GCTGCCAGAAACCCACGTCATG	430	Detecting CRISPR/Cas9 construct
<i>Cas9</i> -F <i>Cas9</i> -R	AGGAGACTATCACCCCTTGGAAAC TTGAAGGTAAGAGAGTCATCGTGG	706	Detecting CRISPR/Cas9 construct

2.6. Grain Trait Examination of the *mtl* Mutants

At maturity, we collected the SSR, grain length (GL), grain width (GW), and thousand-kernel weight (TKW) in the self-pollinated grains of the *mtl* mutants or the cross-pollinated F₁ hybrid grains between “Fielder” and each *mtl* mutant. The SSR was expressed as grain number versus total florets in the sampled spikes. Ten grains were randomly selected from normal grains (NG) and ELG of each material for the determination of GL and GW, and the measurement was repeated for three times.

2.7. Observation of Starch Granules and Protein Bodies in Wheat Grains

To study dynamic change of starch granule (SG) and protein bodies (PB) in wheat immature grains, those with or without embryos in the middle region of a spike were collected at 9, 12, 15, 18, and 23 DPA and then observed under a transmission electron microscope (TEM). Ultrathin sections were prepared by adapting a method from Zhu et al. [35]. In brief, immature grains were sectioned transversely into 1–2 mm pieces, fixed in 2.5% (*v/v*) glutaraldehyde (pH 7.2) for 24 h, and washed six times with 0.1 M PB solution (pH 7.2). Afterwards samples were fixed in 1% osmic acid for 2 h, rinsed six times with PB solution, dehydrated with a serial of ethanol solution (from 30% to 50%, 70%, 90%, and 100%) and with 100% acetone, and infiltrated with 50% and 70% LR White resin each for 3 h and 100% LR White resin overnight. Finally, the samples were polymerized and sectioned for TEM observation.

2.8. Determination of Total Starch and Amylose Contents

The mature and ELG samples of the *mtl* mutants were ground to powder and filtered through a 100 mesh sieve, and stored in a low humidity cabinet. The total starch content was determined by colorimetry [36]. Namely, 100 mg sample was mixed with ethyl alcohol, placed at 70 °C for 2 h, and centrifuged at 12,000 rpm for 10 min. The sample pellet was then soaked in KOH, oscillated in an ice bath for 20 min, and mixed with 1.2 M sodium acetate buffer and starch glucoside enzyme at 50 °C for 30 min. The reaction mix was added up to 100 mL with distilled water; 0.1 mL of the mix was then added to 3 mL glucose oxidase/ peroxidase (GOPOG) and maintained at 50 °C for 20 min. The 510-nm absorption of the reaction mix was measured using a full wavelength multifunctional microplate analyzer (Thermo Scientific, Multiskan Go, Waltham, MA, USA). The test was set with three biological replicates.

Amylose content was determined using a method from Wang et al. [36]. Ten milligram flour samples were mixed with 100% alcohol and 1 M NaOH, and incubated in boiling water for 10 min. The supernatant was taken and mixed with acetic acid and potassium iodide solutions. The reaction was added up to 10 mL with distilled water. The 620-nm absorption of the reaction mix was determined using a full wavelength multifunctional microplate analyzer (Thermo Scientific) and used to calculate the content of amylose. The test was performed with three biological replicates.

2.9. Investigation of Starch Granule Morphology

Starch granule morphology was imaged using a method from Zhou et al. [37]. One hundred milligram starch was mounted on a scanning electron microscope (SEM) brass stub and coated with gold, and then observed under a SEM (Zeiss Merlin Compact, Oberkochen, Germany).

2.10. Quantification of the Gluten and Non-Gluten Contents

Albumins, globulins, gliadins, and glutenins contents were measured using a modified approach [38]. Half a gram of grain powder was mixed well with 5 mL distilled water, oscillated at 220 rpm for 30 min, and centrifugated at 4000 rpm for 15 min. The supernatant was transferred into a container for albumins extraction. The remaining precipitation was dissolved with 5 mL distilled water, then oscillated at 220 rpm for 30 min and centrifugated at 4000 rpm for 15 min. Finally, the supernatant was added up to 50 mL with distilled water and used to measure the albumin content.

Five milliliters of 10% NaCl, then 70% ethyl alcohol, and then 0.2% NaOH were added sequentially to the above precipitation to extract globulin, gliadins, and glutenins. The oscillation and centrifugation steps were performed as described for albumin extraction. The supernatants were diluted with 10% NaCl, 70% ethyl alcohol, and 0.2% NaOH to 50 mL and then used for measurement.

2.11. Statistical Analysis

Data analysis was performed using GraphPad Prism version 8.0.2 (GraphPad Software Inc., La Jolla, CA, USA) and IBM spass Statistics (version 19.0). The criterion for statistical significance was set at * $p < 0.05$, ** $p < 0.01$ and *** $p < 0.001$, respectively. The standard error of the mean (SE) was based on three biological replicates.

3. Results

3.1. Induction of Wheat Haploid Seeds in *mtl* Mutants

Haploid seeds were determined by chromosome numbers and guard cell length among self- and cross-pollinated grains of the tested *mtl* mutants. Diploid plants had 42 chromosomes and the guard cells were in average 70.71 μm in length. Haploid plants had 21 chromosomes and their guard cells were relatively smaller, in average 47.37 μm in length (Figure 1a–d). In a cross design, the *mtl* mutants that also carried homozygous *bar* and *Cas9* genes were used as pollen donors (male parents); the derived haploid plants were negative for both *bar* and *Cas9*, indicating that the haploid DNA was from the female gametes; however, both *bar* and *Cas9* were detected in the derived diploid plants (Figure 1e,f). For *mtl-A*, only diploid plants were obtained, 52 and 43 from self-pollination and a cross-pollination with non-mutants as female, respectively. For *mtl-AD*, seven and six haploid plants were identified in 89 and 66 grains from self-pollination and cross-pollination, representing HIR rates of 7.8% and 9.1%, respectively (Table 2). In *mtl-BD*, there were a HIR of 15.6% in the self-pollinated grains and a HIR of 13.0% in its cross-pollinated grains when using non-mutant as female parents (Table 2). In the progenies of the self- and cross-pollinated combinations of mutant *mtl-ABD*, the haploid induction frequencies were 13.9% and 14.1%, respectively (Table 2). Therefore, the *mtl-A* mutation has no effect on haploid induction; mutations *mtl-BD* and *mtl-ABD* are similar on haploid induction, but both had stronger effect than *mtl-AD*. The mutations *mtl-AD*, *mtl-BD* and *mtl-ABD* each had a similar haploid induction effect between the self- and cross-pollinated populations.

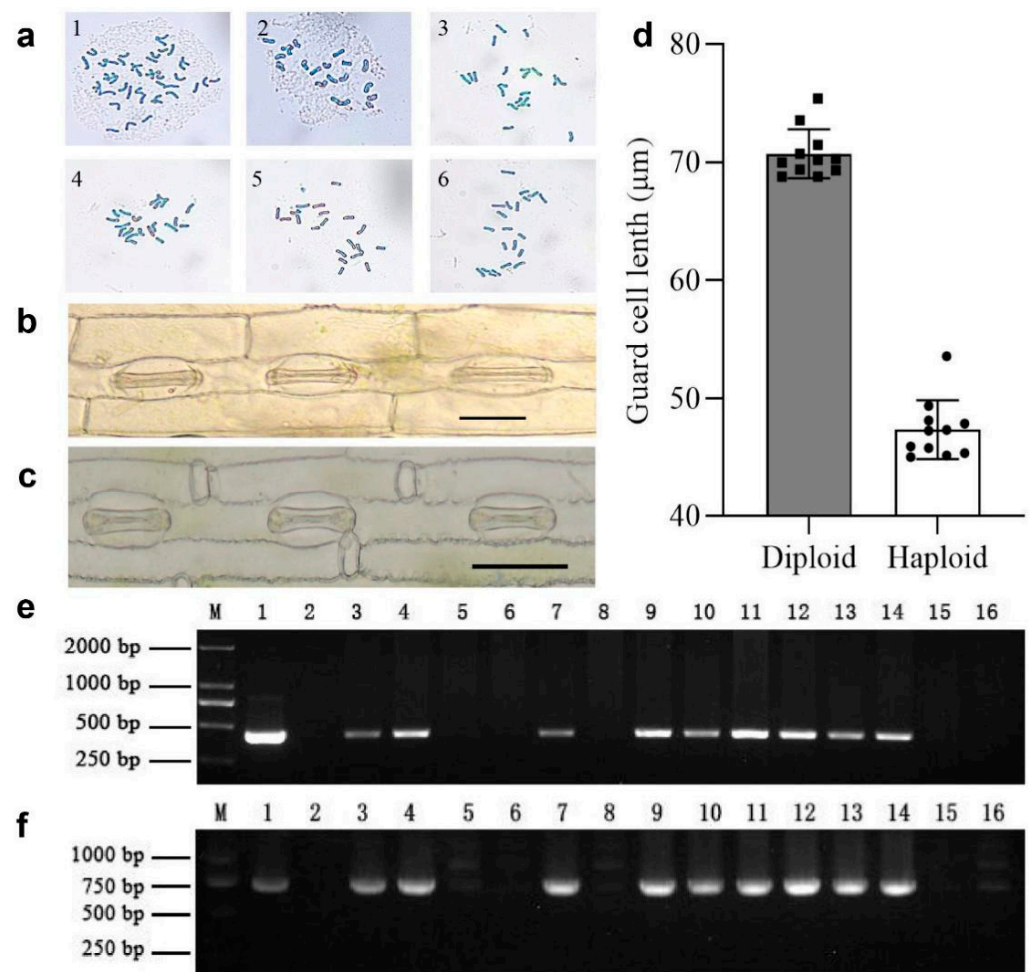


Figure 1. Identification of wheat haploid plants in the *mtl* progenies. (a1) Diploid plants with 42 chromosomes; (a2–a6) Haploid plants with 21 chromosomes; (b) Guard cells of diploid plants, scale bar = 50 μm; (c) Guard cells of haploid plants, scale bar = 50 μm; (d) The guard cell length of diploid and haploid plants, in which the square and round represented individual data point of diploid and haploid plants, respectively; (e,f) Specific amplifying products of F₁ hybrids, M: DL2000 DNA marker; (e1,f1): Positive control plants containing *bar* and *Cas9* genes; (e2,f2): Fieder (negative control); (e3–e16): and (f3–f16): F₁ hybrids of Fieder × *mtl* mutants (the specific bands of *bar* and *Cas9* genes were amplified in diploid samples not in haploid samples).

Table 2. Wheat seed setting rate, haploid induction rate, and embryoless grain analysis in the self- and cross-pollinated combinations of the *mtl* mutants.

Female Parents	Crossing Type or Male Parent	Seed Setting Rate (%)	Haploid Induction Rate (%)	Number of Normal Grains	Number of Embryoless Grains	Frequency for Embryoless Grains (%)
<i>mtl-A</i>	⊗ ^a	96.22	0	1289	0	0
<i>mtl-AD</i>	⊗	52.94	7.8	814	252	23.6
<i>mtl-BD</i>	⊗	39.47	15.6	934	261	21.8
<i>mtl-ABD</i>	⊗	32.41	13.9	1124	356	24.1
Fielder	<i>mtl-A</i>	89.97	0	529	1	0.2
Fielder	<i>mtl-AD</i>	28.06	9.1	142	47	24.9
Fielder	<i>mtl-BD</i>	27.82	13.0	158	55	25.8
Fielder	<i>mtl-ABD</i>	25.71	14.1	193	73	27.4

^a Self-pollinated.

3.2. Wheat Grain Measurements in *mtl* Mutants

Mutant grains at different filling stage were categorized into four classes: (1) NG with embryo and endosperm (either haploids or diploids, Figure 2a); (2) ELG with endosperm but missing an embryo (Figure 2b); (3) EnLG with an embryo but missing endosperm (either haploids or diploids, Figure 2c); (4) aborted grains without embryo and endosperm (Figure 2d). The embryos of the EnLG class were rescued in vitro culture and 26 plants were obtained, among which nine plants were haploids and the remaining plants were diploids (Figure 3a–c).



Figure 2. Wheat grain morphology of the *mtl* progenies. (a) Normal grains with embryo and endosperm; (b) Embryoless grains with endosperm only; (c) Endospermless grains, in which most ones had defective embryos and a few ones had normal embryos; (d) Seedcoat grains without both embryo and endosperm.

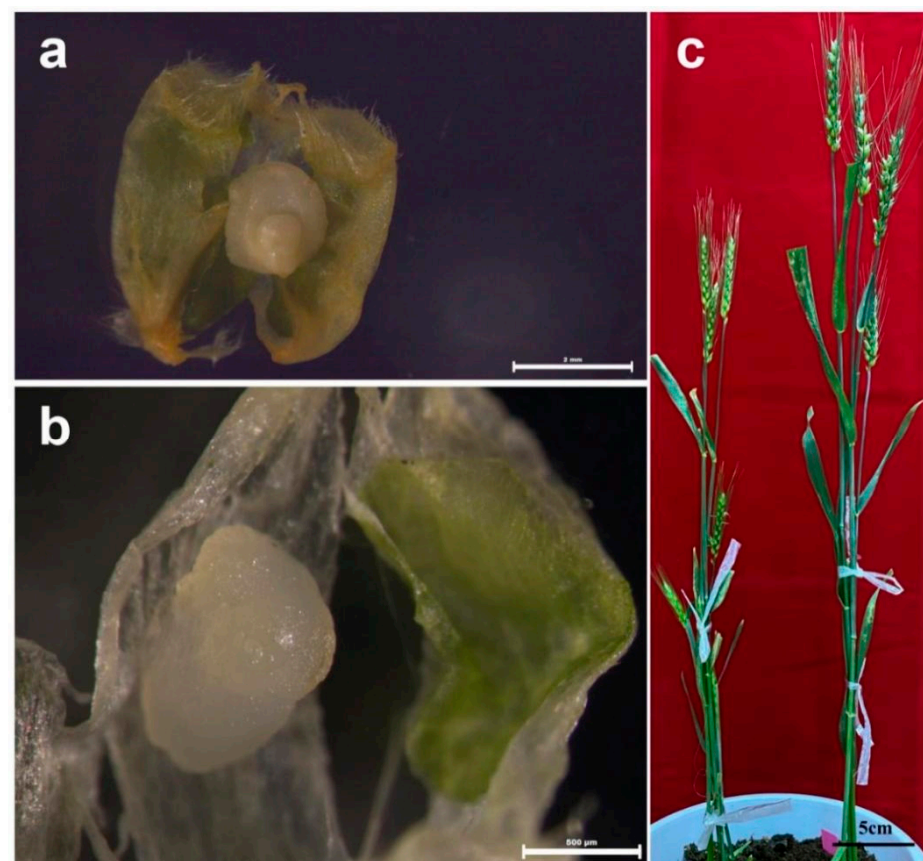


Figure 3. Immature endospermless wheat grains and in vitro rescued embryos of the *mtl* mutants. (a) An endospermless grain with normal embryo, scale bar = 2 mm; (b) An endospermless grain with defective embryo, scale bar = 500 μm; (c) Haploid plant (left) and diploid plant (right) derived from endospermless grains, scale bar = 5 cm.

The EnLG were not counted into total grains at maturity. In average, the embryo abortion rates were 21.8–24.1% and 24.9–27.4% in the self- and cross-pollinated grains in all *mtl* mutants, respectively. For *mtl-A*, there was no ELG in both self- and cross-pollinated progenies, and the SSR were 96.2% and 90%, respectively. However, the SSR for *mtl-AD*, *mtl-BD*, and *mtl-ABD* were 52.9%, 39.5%, and 32.4% in the self-pollinated spikes, and 28.1%, 27.8%, and 25.7% in cross-pollinated spikes (Table 2). Therefore, the *mtl-A* mutation has no effect on embryo development and SSR (Table 2).

How the embryo abortion affects grain development was studied using self-pollinated mature grains of the *mtl* mutants and their WT. There was no significant difference between ELG and NG in GL, GW, and TKW for each mutant group. However, these grain measures in *mtl-AD*, *mtl-BD*, and *mtl-ABD* were all significantly higher than that in *mtl-A* and WT (Figure 4a–h; Table 3). Likely, an embryo is not essential for grain development in wheat.

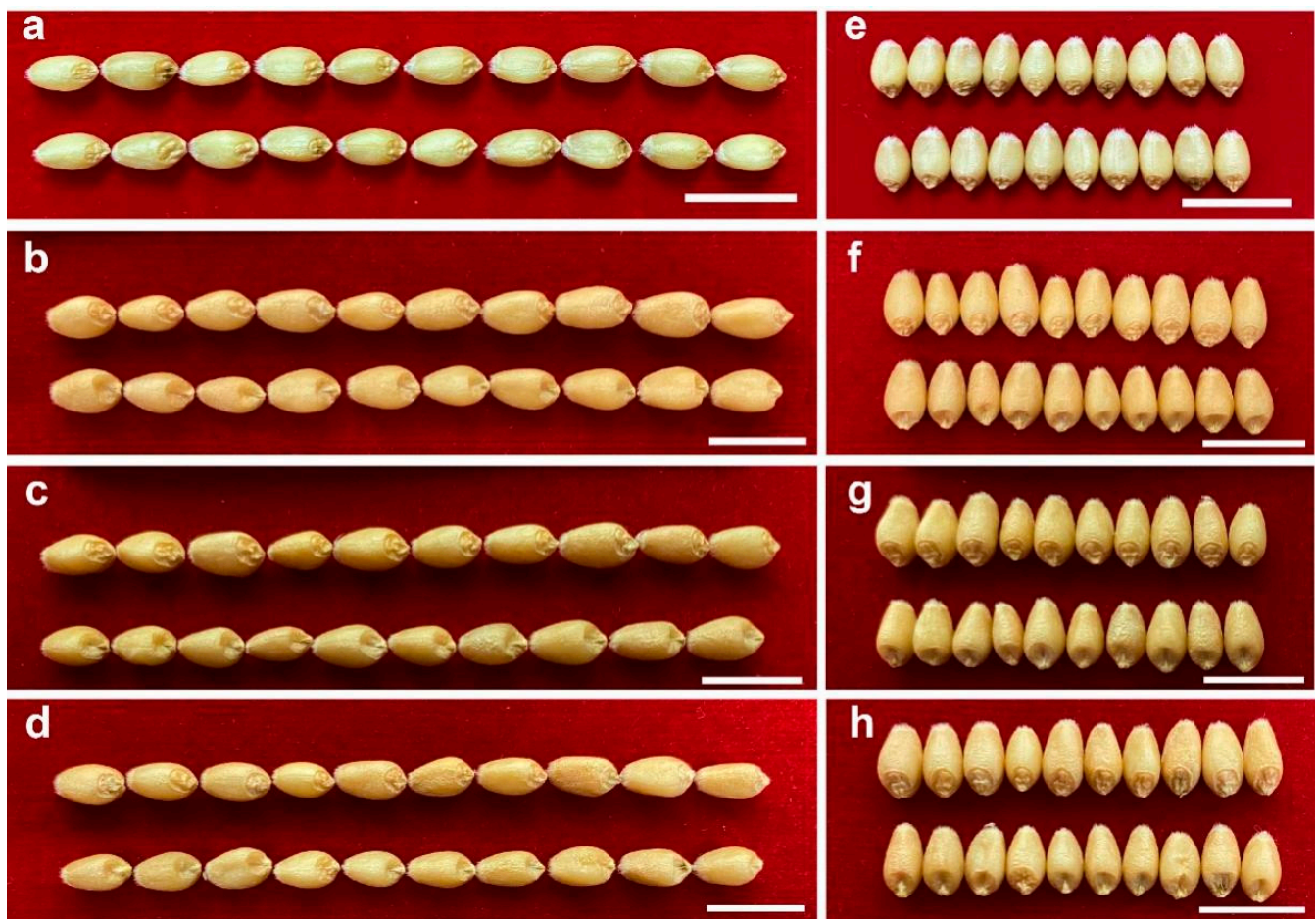


Figure 4. Wheat grain features of the embryoless and normal grains of the *mtl* mutants. (a,e) Comparison on grain length and width between wild-type (upper line) and *mtl-A* (lower line); (b–d) Comparison on grain length between embryoless grain (lower line) and normal grains (upper line) from *mtl-AD*, *mtl-BD*, and *mtl-ABD*; (f–h) Comparison on grain width between embryoless grains (lower line) and normal grains (upper line) from *mtl-AD*, *mtl-BD*, and *mtl-ABD*. Scale bar = 1 cm.

Table 3. Morphology of the normal and embryoless wheat grains of the *mtl* self-pollinated progenies.

Female Parents	Grain Length of Normal Grains (mm)	Grain Length of Embryoless Grains (mm)	Grain Width of Normal Grains (mm)	Grain Width of Embryoless Grains (mm)	TKW for Normal Grains (g)	TKW for Embryoless Grains (g)
Fielder	6.9 ± 0.14	—	3.5 ± 0.02	—	42.53	—
<i>mtl-A</i>	7.0 ± 0.06	—	3.5 ± 0.05	—	42.62	—
<i>mtl-AD</i>	7.3 * ± 0.01	7.2 * ± 0.01	3.9 * ± 0.06	4.0 * ± 0.08	48.92	48.25
<i>mtl-BD</i>	7.3 * ± 0.01	7.2 * ± 0.03	4.0 * ± 0.01	3.9 * ± 0.04	47.32	47.07
<i>mtl-ABD</i>	7.3 * ± 0.04	7.2 * ± 0.06	3.9 * ± 0.02	3.8 * ± 0.01	47.27	46.53

TKW Thousand-kernel weight. Significance was set at * $p < 0.05$.

3.3. Wheat Embryo Abortion in the *mtl-ABD* Mutant

The embryo abortion, with an average rate of 25%, was common in the *mtl* double and triple mutants. The dynamic change of embryo abortion was studied by examining ELG ratio at different DPA in the *mtl-ABD* mutant. The ELG frequency was consistent during grain development (Table 4), and the frequencies for ELG were 28.1, 30.1, 30.9, 28.4, 26.4 and 27.6% at different DPA (Table 4). We believe that embryos aborted as early as 9 DPA and most likely at the beginning of an embryo development.

Table 4. Dynamic change of embryo lethality during wheat grain filling period in the triple *mtl-ABD* mutant.

Days Post Anthesis (d)	Number of Normal Grains	Number of Embryoless Grains	Frequency for Embryoless Grains (%)
9	287	112	28.1
12	221	95	30.1
15	230	103	30.9
18	229	91	28.4
23	234	84	26.4
28	243	93	27.6

3.4. Effect of Embryo Abortion on Endosperm Structure

How embryo abortion affects SG and PB was studied by TEM-based scanning of immature grains from the *mtl-ABD* mutant at different development stage. The SG accumulation in endosperm started as early as 9 DPA, as well as the PB; they gradually increased in size and quantity in both the embryo abortion and embryo normal grains of the mutant (Figure 5a–j). However, the morphology of SG and PB showed no significant difference between the embryo abortion and embryo normal grains. We speculated that the embryo abortion does not affect the morphology of SG and PB in the endosperm of the triple mutant.

3.5. Effect of Wheat Embryo Abortion on Starch Content and Starch Granule Composition

To further clarify how embryo abortion affects nutrient accumulation in mature grains, total starch and amylose in mature ELG and NG were determined for three *mtl* mutant groups: *mtl-AD*, *mtl-BD*, and *mtl-ABD*. The total starch content in NG was higher than that in ELG in all three mutant groups, whereas the amylose content had a reverse trend. ANOVA analysis revealed that the total starch content was significantly different between the ELG and NG in *mtl-AD*, *mtl-BD*, and *mtl-ABD*, and the amylose content was significantly different between ELG and NG in *mtl-AD* and *mtl-BD*, but not in *mtl-ABD* ($p = 0.3290$) (Figure 6a,b).

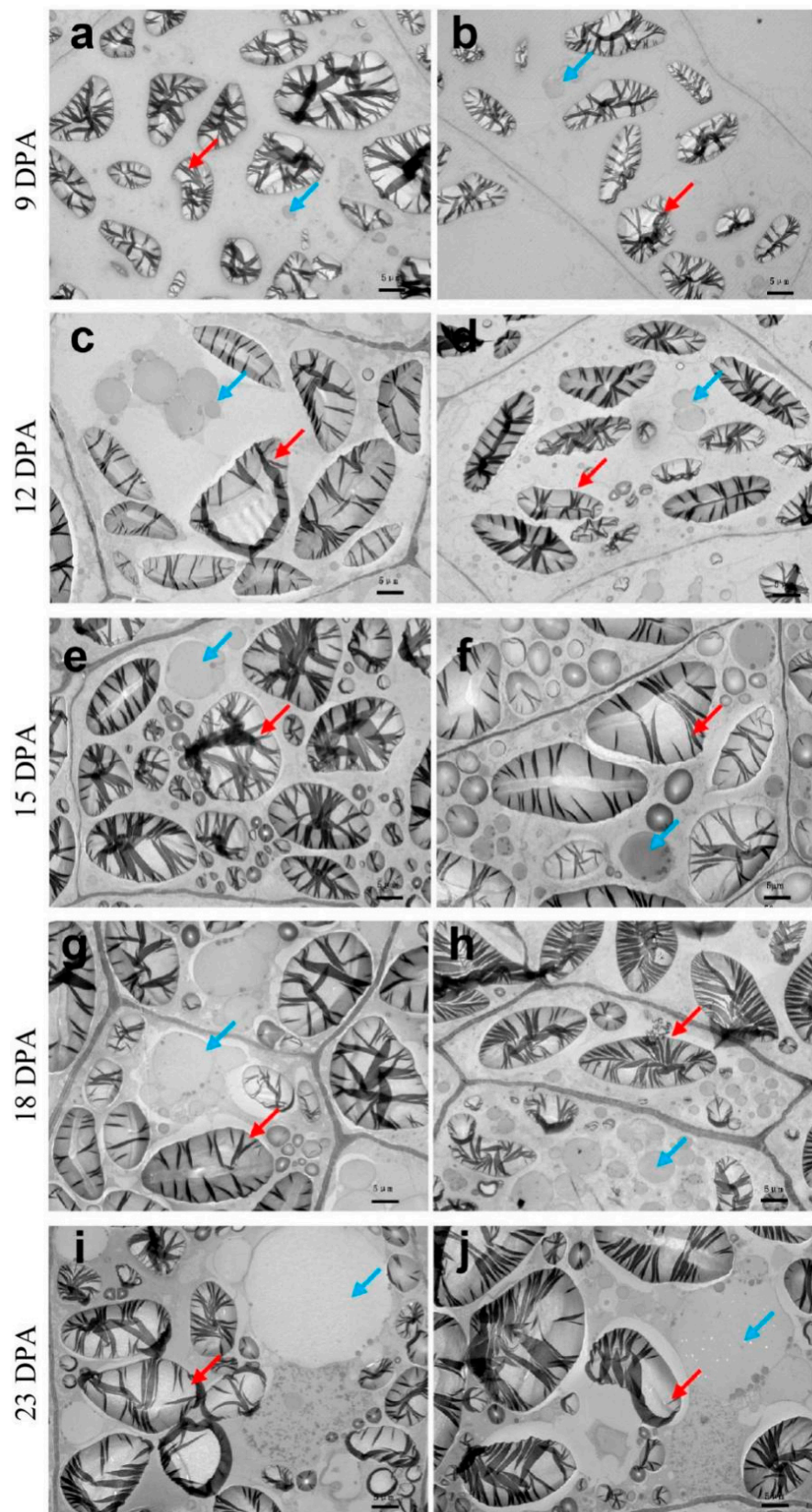


Figure 5. Starch granule and protein body in normal and embryoless wheat grains during grain-filling in the *mtl* mutants. (a,c,e,g,i) The dynamic change of starch granule (SG) and protein body (PB) in normal grains; (b,d,f,h,j) The dynamic change of SG and PB in embryoless grains. The SG were highlighted by red arrows, and the PB were highlighted by blue arrows. Scale bar = 5 μm.

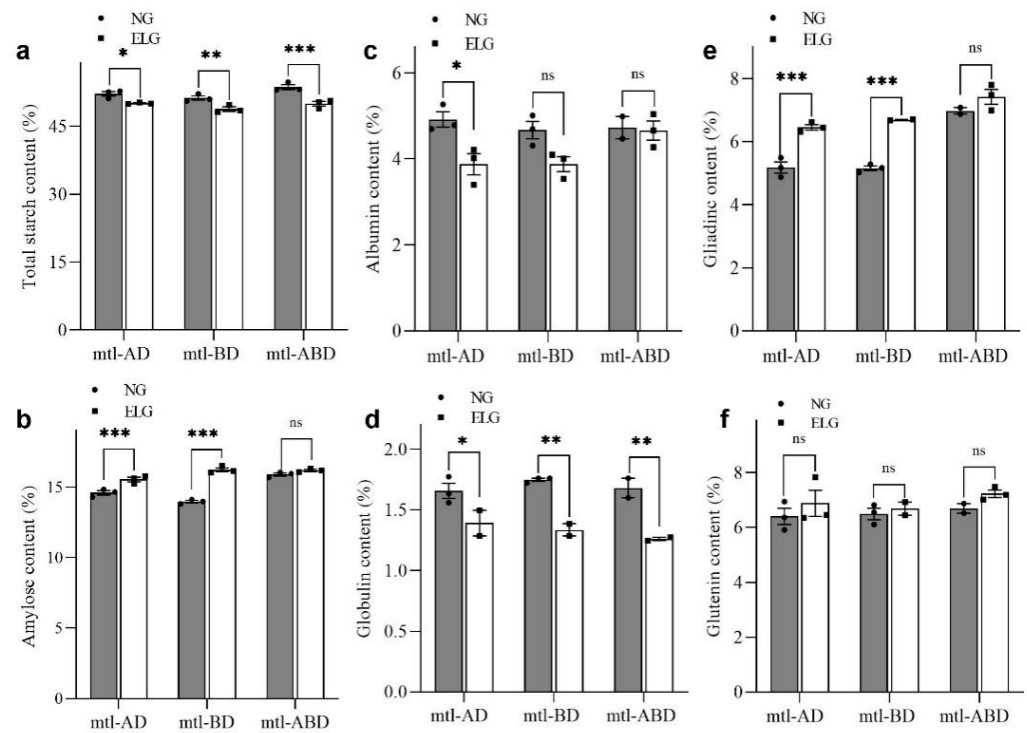


Figure 6. Nutrient accumulation in embryoless wheat grains of the *mtl* mutants. (a–f) Contents of starch, amylose, albumin, globulin, gliadin, and glutenin in the *mtl* grains. *, **, *** and ns indicated significance at $p < 0.05$, $p < 0.01$, $p < 0.001$ and no significance in order.

Regarding to the A-type granules (flattened, 10–35 μm in diameter) and B-type granules (round, 1–10 μm in diameter), there was no obvious morphological difference on diameter and shape between ELG and NG in all three mutant groups (Figure 7a–h). Thus, the embryo abortion might have no effect on SG composition but have a slight effect on starch accumulation.

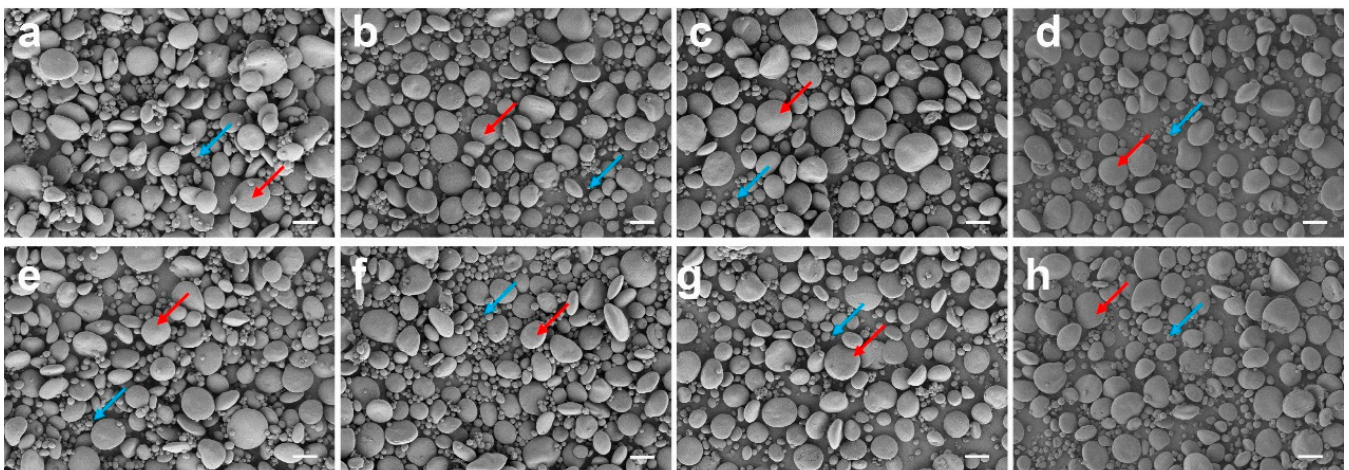


Figure 7. Starch granule in mature wheat grains of the *mtl* mutants. (a) “Fielder” (WT); (b–d) Normal grains from *mtl-AD*, *mtl-BD*, and *mtl-ABD*; (e) Normal grains from *mtl-A*; (f–h) Embryoless grains from *mtl-AD*, *mtl-BD*, and *mtl-ABD*. The red arrows indicated A-type starch granules and blue arrows indicated B-type starch granules, scale bar = 20 μm .

3.6. Effect of Wheat Embryo Abortion on Grain Storage Protein Composition

The albumin content in ELG was lower than that in NG in the *mtl-AD*, *mtl-BD*, and *mtl-ABD* mutants. For example, ELG of *mtl-AD* had a reduction proportion of 21.2%

($p < 0.05$) (Figure 6c). As for the globulin content, the reduction proportions in ELG in relative to NG were 15.9%, 23.5%, 24.9% in *mtl-AD* ($p = 0.0366$), *mtl-BD* ($p = 0.0031$), and *mtl-ABD* ($p = 0.0049$), respectively (Figure 6d). The gliadin content in ELG was significantly increased ($p < 0.001$) in *mtl-AD* (24.6%) and *mtl-BD* (29.7%), when compared with those in NG of the same mutant group (Figure 6e). The glutenin content in the ELG was slightly higher than that in the NG in the three types of mutants, but no significant difference was detected ($p = 0.6051, 0.9661, 0.5984$) (Figure 6f). It appears that the embryo abortion had some effects on protein accumulation in wheat grains.

4. Discussion

4.1. The *mtl-A* Mutation Has No Effect on Wheat Grain Phenotype

The maize *qhir1* mutant has three types of kernels after self- and cross-pollination: (1) normal seeds as haploids or diploids, (2) endosperm abortion (EnA) seeds with shrunken endosperm, (3) embryo abortion (EmA) seeds with endosperm but lacking an embryo. The *qhir1* gene (or called *ZmPLA1*) induces haploid seeds in maize [27,39]. Here, the self- and cross-pollinated grains of the tested *mtl* mutants except *mtl-A* were associated with approximately 25% ELG and low SSR. Although it has been reported that knockout of the *PLA1/MTL* gene in wheat induced haploid seeds [30,31], it is still unclear how *pla1/mtl* mutations impact grain traits and the grain storage proteins.

For HIR, there was a sequential decrease from *mtl-ABD*, to *mtl-BD*, and to *mtl-AD* in the self- and cross-pollinated progenies (Table 2). For GL, GW, TKW, SSR, and embryo or endosperm development, the *mtl-A* had no effect, but mutations occurred to other genomes (B and D) significantly impacted those traits (Figure 4; Tables 2 and 3).

4.2. Independence between Wheat Embryo and Endosperm Development

There are contradicting views on how embryo and endosperm work together to form a seed. Some experts believe that embryo and endosperm interact with each other; others think the embryo and endosperm development are independent. In maize defective kernel (*dek*) mutant, a defective endosperm can be improved when there is an intact embryo, and vice versa, which implies dependence between embryo and endosperm [40]. On the other hand, in vitro fusion between the central nucelli and the sperm cell could form endosperm cells in maize [41].

When the maize HI lines were used as males for cross-pollination, endosperm developed well in some ELG grains; apparently, the endosperm development can be independent of an embryo [39]. In this study, there was no difference in SG and PB between ELG and normal grains (Figure 5a–j), as well as the GL, GW, and TKW traits (Figure 4a–h; Table 3). In contrast, embryos developed in some EnLG among the self-pollinated progenies, and this type of embryos could be rescued by tissue culture. Apparently, embryo and endosperm can be independently developed in wheat.

The contents of amylose, gliadin, and glutenin in ELG were higher than those in NG in the *mtl* mutants, while total starch, albumin, and globulin had a reverse pattern (Figure 6a–e). Therefore, embryo abortion should have no effect on grain morphology, but might affect nutrient accumulation in the endosperms of the *mtl* mutants. Gliadins and glutenins are primarily related to the extensibility and elasticity of dough which have a major influence on flour processing quality [16]. Therefore, we speculated that the ELG might have some influence on baking quality.

In self- and cross-pollination grains from the maize HI lines, embryos occurred among the endosperm defective grains. It was speculated that these embryos should be haploids, and an irregular embryogenesis might impede the endosperm development [39]. Here, we also obtained embryos in the endosperm defective grains in the *mtl-ABD* mutant, but only one-third of them were haploids (Figure 3a–c). Clearly, both haploid and diploid embryos occurred in the endosperm defective grains of the *mtl* mutants. However, further studies are needed to uncover the underlying mechanisms of this phenomenon.

4.3. Endosperm Origin in Wheat Embryoless Grains of the *mtl* Mutants

In maize, the endosperm forms in the maize defective kernels (EnA and EmA), which are probably due to a double fertilization without chromosome elimination [39]. The endosperm formation in the wheat ELG might also be from a double fertilization without chromosome elimination. However, in *Arabidopsis*, the *FIE*, *FIS* and *F644* genes mainly inhibit endosperm development and promote embryo development before fertilization. When these genes were mutated in *Arabidopsis*, the central cells could divide without fertilization to form a diploid endosperm, and the mutation mainly transmits through the female gametophyte and has no effect on the male gametophyte [42–44]. The *MTL* gene encodes a pollen-specific phospholipase, expresses in the male gametophyte. Embryoless grains were found not only in the self-pollinated progenies of *mtl* mutants, but also in the cross-pollinated progenies when the *mtl* mutants (excluding *mtl-A*) were used as male parents. In wheat, the endosperm in ELG might be diploid and should be derived from unfertilized central cells.

In higher plants, the gametophyte and sporophyte differ greatly in morphology. There are tons of regulatory proteins governing plant growth and development, which functions are to fine tune the gametophyte and sporophyte developmental pathways [17,43,45]. Here, there were more than 20% ELG in the self- or cross-pollinated progenies of *mtl-AD*, *mtl-BD*, and *mtl-ABD* (Tables 2 and 4). Likely, the *MTL* from the genome B and/or D might regulate the expression of its/their downstream gene(s) controlling the fertilization of male gametophytes, which further affect the proliferation and growth of maternal egg cells or central cells during or after fertilization. This hypothesis is consistent with the “kinship” theory in which parental genomes conflict each other, leading to gene imprinting and different gene expression profiles imposed by each parental genome [45].

4.4. Rapid Screening of the Wheat Haploids Induced by the *mtl* Mutations

In recent years, haploids have been efficiently induced by interrupting *PLA1*, *MTL*, *DMP*, *CENH3*, and *PLD3* genes in maize, rice, *Arabidopsis*, wheat, foxtail millet, and tomato using CRISPR/Cas9 technology [28–31,46–52]. As for plant double haploid breeding, a limiting step is the generation of haploid seeds. Gene editing represent a new path to fast screen haploid grains or seedlings from the F₁ hybrids. However, there is no morphological markers for the haploid grains in the current gene editing based populations. Even though the haploids can be identified by flow cytometry [53], chromosome number [31], and guard cell size [31], those methods are time-consuming or expensive cost. Fluorescent proteins were used to identify haploid and diploid seeds, for which the green fluorescent protein (*eGFP*) and red fluorescent protein (*DsRED*) were expressed by the maize embryo specific promoters and the barley endosperm specific promoters, respectively [54]. However, fluorescent proteins must be visualized by specific equipment. In this study, we used the *bar* and *Cas9* gene markers to identify the haploids in a cross-pollination design where the *mtl* mutants were used as male parents; this method is cost effective and highly efficient (Figure 1e,f). It appeared that haploid plants were originated from unfertilized female gametes and were negative for both *bar* and *Cas9*, however the diploid plants were from zygotes containing *bar* and *Cas9*. We are also interested in developing visual markers to identify the haploid plants.

5. Conclusions

The *mtl-AD*, *mtl-BD*, and *mtl-ABD* were effective for haploid induction in the self- and cross-pollinated progenies. Haploids were quickly and accurately identified from the F₁ hybrids that involved the use of *mtl* mutants as male parents. *mtl-A* had no effect on HI, SSR, GL, GW, TKW, and embryo or endosperm abortion, but *mtl-AD*, *mtl-BD* and *mtl-ABD* had enormous changes on these traits both in the self- and cross-pollinated grains. In relative to NG, ELG contained higher levels of amylose, gliadin and glutenin but lower levels of total starch, albumin, and globulin in the self-pollinated progenies from *mtl-AD*,

mtl-BD, and *mtl-ABD*. Embryos likely aborted at the beginning of their initiation, and it might affect nutrient accumulation and bread-baking quality in wheat.

Author Contributions: The experiment was conceived by X.Y. and Z.L. (Zichao Li). H.T., S.Z., M.Y. and Y.Y. made crosses, investigated seed setting rate, grain morphological characteristics, and performed haploid plant identification. H.T., S.Z., K.W., Y.C. and Z.L. (Zhisha Lin) detected the development progress of embryoless grains. H.T., M.Y. and K.W. did the rescue culture of the isolated developing embryos from the endospermless grains. H.T., K.W. and Y.Q. conducted grain starch and storage protein analysis. Z.L. (Zhisha Lin) and L.D. cultured and managed wheat materials. H.T., S.Z., K.W., X.Y. and Z.L. (Zichao Li) analyzed all the data. The manuscript was drafted by H.T., X.Y. and Z.L. (Zichao Li); Supervision, D.F., Z.L. (Zichao Li) and X.Y.; D.F., Z.L. (Zichao Li) and X.Y. revised the manuscript. All authors have read and agreed to the published version of the manuscript.

Funding: This research was financially supported in part by the Key Research and Development Program from the Science and Technology Department of Ningxia Hui Autonomous Region (2019BBF02020) and the Agricultural Science and Technology Innovation Program from the Chinese Academy of Agricultural Sciences (S2022ZD03).

Institutional Review Board Statement: No applicable.

Informed Consent Statement: This manuscript has no applicable.

Data Availability Statement: No applicable.

Acknowledgments: We sincerely thank Qian Wei and Jianan Wu at the Core Facility Platform, Institute of Crop Sciences, Chinese Academy of Agricultural Sciences for their assistance with TEM analysis.

Conflicts of Interest: This manuscript has no financial or non-financial competing interests.

Abbreviations

CRISPR/Cas9, clustered regularly interspaced short palindromic repeats associated protein 9; DNA, deoxyribonucleic acid; DPA, days post anthesis; ELG, embryoless grain; EnLG, endospermless grain; GL, grain length; GW, grain width; HIR, haploid induction rate; NG, normal grains; PB, protein bodies; PCR, polymerase chain reaction; SG, starch granules; SEM, scanning electron microscope; SSR, seed setting rate; TEM, transmission electron microscope; TKW, thousand kernel weight.

References

- Berger, F.; Hamamura, Y.; Ingouff, M.; Higashiyama, T. Double fertilization-caught in the act. *Trends Plant Sci.* **2008**, *13*, 437–443. [[PubMed](#)]
- Evers, T.; Millar, S. Cereal Grain Structure and Development: Some Implications for Quality. *J. Cereal Sci.* **2002**, *36*, 261–284. [[CrossRef](#)]
- Sabelli, P.A.; Larkins, B.A. The Development of Endosperm in Grasses. *Plant Physiol.* **2009**, *149*, 14–26. [[CrossRef](#)] [[PubMed](#)]
- Conlon, I.; Raff, M. Size Control in Animal Development. *Cell* **1999**, *96*, 235–244. [[CrossRef](#)]
- Crickmore, M.A.; Mann, R.S. The control of size in animals: Insights from selector genes. *BioEssays* **2008**, *30*, 843–853. [[CrossRef](#)]
- Food and Agriculture Organization of the United Nations (FAO). *World Food Situation: FAO Cereal Supply and Demand Brief*; Food and Agriculture Organization of the United Nations (FAO): Rome, Italy, 2016.
- Barron, C.; Surget, A.; Rouau, X. Relative amounts of tissues in mature wheat (*Triticum aestivum* L.) grain and their carbohydrate and phenolic acid composition. *J. Cereal Sci.* **2007**, *45*, 88–96. [[CrossRef](#)]
- Hurkman, W.J.; McCue, K.; Altenbach, S.B.; Korn, A.; Tanaka, C.K.; Kothari, K.M.; Johnson, E.L.; Bechtel, D.B.; Wilson, J.D.; Anderson, O.D.; et al. Effect of temperature on expression of genes encoding enzymes for starch biosynthesis in developing wheat endosperm. *Plant Sci.* **2003**, *164*, 873–881. [[CrossRef](#)]
- Shewry, P.R.; Napier, J.A.; Tatham, A.S. Seed storage proteins—structures and biosynthesis. *Plant Cell.* **1995**, *7*, 945–956.
- Ball, S.G.; Morell, M.K. From Bacterial Glycogen to Starch: Understanding the Biogenesis of the Plant Starch Granule. *Annu. Rev. Plant Biol.* **2003**, *54*, 207–233. [[CrossRef](#)]
- Botticella, E.; Sestili, F.; Hernandez-Lopez, A.; Phillips, A.; Lafiandra, D. High resolution melting analysis for the detection of EMS induced mutations in wheat *Sb1* genes. *BMC Plant Biol.* **2011**, *11*, 156.

12. Li, J.; Jiao, G.; Sun, Y.; Chen, J.; Zhong, Y.; Yan, L.; Xia, L. Modification of starch composition, structure and properties through editing of TaSBEL1a in both winter and spring wheat varieties by CRISPR/Cas9. *Plant Biotechnol. J.* **2021**, *19*, 937–951.
13. Evers, A.D. Scanning Electron Microscopy of Wheat Starch. III. Granule Development in the Endosperm. *Starch* **1971**, *23*, 157–162. [[CrossRef](#)]
14. Evers, A.D. The Size Distribution Among Starch Granules in Wheat Endosperm. *Starch* **1973**, *25*, 303–304. [[CrossRef](#)]
15. Morrison, W.; Gadan, H. The amylose and lipid contents of starch granules in developing wheat endosperm. *J. Cereal Sci.* **1987**, *5*, 263–275. [[CrossRef](#)]
16. Shevkani, K.; Singh, N.; Bajaj, R.; Kaur, A. Wheat starch production, structure, functionality and applications—a review. *Int. J. Food Sci. Technol.* **2016**, *52*, 38–58. [[CrossRef](#)]
17. Faridi, H.; Finley, J.W.; D’Appolonia, B. Improved wheat for baking. *Crit. Rev. Food Sci. Nutr.* **1989**, *28*, 175–209. [[CrossRef](#)]
18. Fiaz, S.; Sheng, Z.; Zeb, A.; Barman, H.N.; Shar, T.; Ali, U.; Tang, S. Analysis of genomic regions for crude protein and fractions of protein using a recombinant inbred population in rice (*Oryza sativa* L.). *J. Taibah Univ. Sci.* **2021**, *15*, 579–588.
19. Snyder, H. *The Proteins of the Wheat Kernel*; American Association for the Advancement of Science: Washington, DC, USA, 1907.
20. Dupont, F.M.; Vensel, W.H.; Tanaka, C.K.; Hurkman, W.J.; Altenbach, S.B. Deciphering the complexities of the wheat flour proteome using quantitative two-dimensional electrophoresis, three proteases and tandem mass spectrometry. *Proteome Sci.* **2011**, *9*, 10. [[CrossRef](#)]
21. Loussert, C.; Popineau, Y.; Mangavel, C. Protein bodies ontogeny and localization of prolamin components in the developing endosperm of wheat caryopses. *J. Cereal Sci.* **2008**, *47*, 445–456. [[CrossRef](#)]
22. Vensel, W.H.; Tanaka, C.K.; Altenbach, S.B. Protein composition of wheat gluten polymer fractions determined by quantitative two-dimensional gel electrophoresis and tandem mass spectrometry. *Proteome Sci.* **2014**, *12*, 8. [[CrossRef](#)]
23. Tao, H.P.; Kasarda, D.D. Two-Dimensional Gel Mapping and N-Terminal Sequencing of LMW-Glutelin Subunits. *J. Exp. Bot.* **1989**, *40*, 1015–1020. [[CrossRef](#)]
24. Bean, S.R.; Lookhart, G.L. Factors Influencing the Characterization of Gluten Proteins by Size-Exclusion Chromatography and Multiangle Laser Light Scattering (SEC-MALLS). *Cereal Chem.* **2001**, *78*, 608–618. [[CrossRef](#)]
25. Don, C.; Mann, G.; Bekes, F.; Hamer, R. HMW-GS affect the properties of glutenin particles in GMP and thus flour quality. *J. Cereal Sci.* **2006**, *44*, 127–136. [[CrossRef](#)]
26. Shewry, P.R.; D’Ovidio, R.; Lafiandra, D.; Jenkins, J.A.; Mills, E.C.; Békés, F. Wheat grain proteins. In *Wheat: Chemistry and Technology*; American Association of Cereal Chemists: St. Paul, MN, USA, 2009; pp. 223–298.
27. Kelliher, T.; Starr, D.; Richbourg, L.; Chintamanani, S.; Delzer, B.; Nuccio, M.L.; Green, J.; Chen, Z.; McCuiston, J.; Wang, W.; et al. MATRILINEAL, a sperm-specific phospholipase, triggers maize haploid induction. *Nature* **2017**, *542*, 105–109. [[CrossRef](#)] [[PubMed](#)]
28. Liu, C.; Li, X.; Meng, D.; Zhong, Y.; Chen, C.; Dong, X.; Xu, X.; Chen, B.; Li, W.; Li, L.; et al. A 4-bp Insertion at ZmPLA1 Encoding a Putative Phospholipase A Generates Haploid Induction in Maize. *Mol. Plant* **2017**, *10*, 520–522. [[CrossRef](#)] [[PubMed](#)]
29. Yao, L.; Zhang, Y.; Liu, C.; Liu, Y.; Wang, Y.; Liang, D.; Liu, J.; Sahoo, G.; Kelliher, T. OsMATL mutation induces haploid seed formation in indica rice. *Nat. Plants* **2018**, *4*, 530–533. [[CrossRef](#)]
30. Liu, C.; Zhong, Y.; Qi, X.; Chen, M.; Liu, Z.; Chen, C.; Tian, X.; Li, J.; Jiao, Y.; Wang, D.; et al. Extension of the in vivo haploid induction system from diploid maize to hexaploid wheat. *Plant Biotechnol. J.* **2019**, *18*, 316–318. [[CrossRef](#)]
31. Liu, H.Y.; Wang, K.; Jia, Z.M.; Gong, Q.; Lin, Z.S.; Du, L.P.; Ye, X. Editing TaMTL gene induces haploid plants efficiently by optimized Agrobacterium-mediated CRISPR system in wheat. *J. Exp. Bot.* **2020**, *71*, 1337–1349.
32. Du, L.P.; Xu, H.J.; Zhao, L.L.; Zhang, C.X.; Ye, X.G. Identification of ploidy of wheat pollen plants using length of guard cell. *Beijing Agric. Sci.* **1996**, *14*, 10–12. (In Chinese)
33. Li, S.; Wang, J.; Wang, K.; Chen, J.; Wang, K.; Du, L.; Ye, X. Development of PCR markers specific to *Dasypyrum villosum* genome based on transcriptome data and their application in breeding *Triticum aestivum*-D. *villosum*#4 alien chromosome lines. *BMC Genom.* **2019**, *20*, 289.
34. Yuan, J.; Guo, X.; Hu, J.; Lv, Z.; Han, F. Characterization of two CENH 3 genes and their roles in wheat evolution. *New Phytol.* **2014**, *206*, 839–851. [[CrossRef](#)]
35. Zhu, J.; Fang, L.; Yu, J.; Zhao, Y.; Chen, F.; Xia, G. 5-Azacytidine treatment and TaPBF-D over-expression increases glutenin accumulation within the wheat grain by hypomethylating the Glu-1 promoters. *Theor. Appl. Genet.* **2018**, *131*, 735–746.
36. Wang, H.; Yang, J.; Zhang, M.; Fan, W.; Firon, N.; Pattanaik, S.; Yuan, L.; Zhang, P. Altered Phenylpropanoid Metabolism in the Maize Lc-Expressed Sweet Potato (*Ipomoea batatas*) Affects Storage Root Development. *Sci. Rep.* **2016**, *6*, 1–15. [[CrossRef](#)]
37. Zhou, T.; Zhou, Q.; Li, E.; Yuan, L.; Wang, W.; Zhang, H.; Liu, L.; Wang, Z.; Yang, J.; Gu, J. Effects of nitrogen fertilizer on structure and physicochemical properties of ‘super’ rice starch. *Carbohydr. Polym.* **2020**, *239*, 116237. [[CrossRef](#)]
38. Zheng, T.; Qi, P.-F.; Cao, Y.-L.; Han, Y.-N.; Ma, H.-L.; Guo, Z.-R.; Wang, Y.; Qiao, Y.-Y.; Hua, S.-Y.; Yu, H.-Y.; et al. Mechanisms of wheat (*Triticum aestivum*) grain storage proteins in response to nitrogen application and its impacts on processing quality. *Sci. Rep.* **2018**, *8*, 11928. [[CrossRef](#)]
39. Xu, X.; Li, L.; Dong, X.; Jin, W.; Melchinger, A.E.; Chen, S. Gametophytic and zygotic selection leads to segregation distortion through in vivo induction of a maternal haploid in maize. *J. Exp. Bot.* **2013**, *64*, 1083–1096.
40. Neuffer, M.G.; Sheridan, W.F. Defective kernel mutants of maize. I. genetic and lethality studies. *Genetics* **1980**, *95*, 929–944. [[CrossRef](#)]

41. Kranz, E.; Von Wieggen, P.; Quader, H.; Lörz, H. Endosperm development after fusion of isolated, single maize sperm and central cells in vitro. *Plant Cell*. **1998**, *10*, 511–524.
42. Ohad, N.; Margossian, L.; Hsu, Y.C.; Williams, C.; Repetti, P.; Fischer, R.L. A mutation that allows endosperm development without fertilization. *Proc. Natl. Acad. Sci. USA* **1996**, *93*, 5319–5324. [[CrossRef](#)]
43. Grossniklaus, U.; Vielle-Calzada, J.P.; Hoepfner, M.A.; Gagliano, W.B. Maternal control of embryogenesis by medea, a Polycomb group gene in Arabidopsis. *Science* **1998**, *280*, 446–450.
44. Ohad, N. Plant development: Parental conflict overcome. *Nature* **2007**, *447*, 275–276. [[CrossRef](#)]
45. Haig, D.; Westoby, M. Parent-Specific Gene Expression and the Triploid Endosperm. *Am. Nat.* **1989**, *134*, 147–155. [[CrossRef](#)]
46. Zhong, Y.; Liu, C.; Qi, X.; Jiao, Y.; Wang, D.; Wang, Y.; Liu, Z.; Chen, C.; Chen, B.; Tian, X.; et al. Mutation of ZmDMP enhances haploid induction in maize. *Nat. Plants* **2019**, *5*, 575–580. [[CrossRef](#)]
47. Kuppup, S.; Ron, M.; Marimuthu, M.P.; Li, G.; Huddleson, A.; Siddeek, M.H.; Terry, J.; Buchner, R.; Shabek, N.; Comai, L.; et al. A variety of changes, including CRISPR/Cas9-mediated deletions, in CENH3 lead to haploid induction on outcrossing. *Plant Biotechnol. J.* **2020**, *18*, 2068–2080. [[CrossRef](#)]
48. Lv, J.; Yu, K.; Wei, J.; Gui, H.; Liu, C.; Liang, D.; Wang, Y.; Zhou, H.; Carlin, R.; Rich, R.; et al. Generation of paternal haploids in wheat by genome editing of the centromeric histone CENH3. *Nat. Biotechnol.* **2020**, *38*, 1397–1401. [[CrossRef](#)]
49. Zhong, Y.; Chen, B.; Li, M.; Wang, D.; Jiao, Y.; Qi, X.; Wang, M.; Liu, Z.; Chen, C.; Wang, Y.; et al. A DMP-triggered in vivo maternal haploid induction system in the dicotyledonous Arabidopsis. *Nat. Plants* **2020**, *6*, 466–472. [[CrossRef](#)]
50. Cheng, Z.; Sun, Y.; Yang, S.; Zhi, H.; Yin, T.; Ma, X.; Sui, Y. Establishing in planta haploid inducer line by edited SiMTL in foxtail millet (*Setaria italica*). *Plant Biotechnol. J.* **2021**, *19*, 1089–1091.
51. Li, Y.; Lin, Z.; Yue, Y.; Zhao, H.; Fei, X.; Liu, C.; Chen, S.; Lai, J.; Song, W. Loss-of-function alleles of ZmPLD3 cause haploid induction in maize. *Nat. Plants* **2021**, *7*, 1579–1588. [[CrossRef](#)] [[PubMed](#)]
52. Zhong, Y.; Chen, B.; Wang, D.; Zhu, X.; Li, M.; Zhang, J.; Chen, M.; Wang, M.; Riksen, T.; Liu, J.; et al. In vivo maternal haploid induction in tomato. *Plant Biotechnol. J.* **2021**, *20*, 250–252. [[CrossRef](#)] [[PubMed](#)]
53. Bohanec, B.; Jakše, M. Variations in gynogenic response among long-day onion (*Allium cepa* L.) accessions. *Plant Cell Rep.* **1999**, *18*, 737–742. [[CrossRef](#)]
54. Dong, L.; Li, L.; Liu, C.; Liu, C.; Geng, S.; Li, X.; Xie, C. Genome editing and double-fluorescence proteins enable robust maternal haploid induction and identification in Maize. *Mol. Plant.* **2018**, *11*, 1214–1217. [[PubMed](#)]